IJCRT.ORG ISSN : 2320-2882

INTERNATIONAL JOURNAL OF CREATIVE RESEARCH THOUGHTS (IJCRT)

An International Open Access, Peer-reviewed, Refereed Journal

Green Detox: Aqueous Extracts Driving Chromium Cleanup from Leather Wastewater

[1]Vanithadevi K, [2]Ramana C, [3]Saran Joseph P, [4]Thamizharasan R, [5]Mutheeswaran M

[1]Assistant Professor, [2,3,4,5] UG STUDENTS

[1,2,3,4,5]DEPARTMENT OF BIOTECHNOLOGY,

[1,2,3,4,5]SALEM COLLEGE OF ENGINEERING AND TECHNOLOGY,

NH-68, Salem-Attur Main Road, Mettupatty, Perumapalayam, Selliamman Nagar,

Salem, Tamil Nadu 636111

Abstract: Industrial effluents from the leather tanning process contain high levels of chromium, posing serious environmental and health hazards. In this study, an aqueous plant extract will be explored as a green, sustainable reducing agent for the removal of chromium from leather industry wastewater. The extract will be analyzed using GC–MS to identify major bioactive compounds responsible for redox activity, and its antioxidant potential will be evaluated to understand its correlation with metal reduction efficiency. The influence of process parameters such as pH, temperature, initial chromium concentration, and contact time will be systematically investigated to optimize the reduction conditions. Kinetic modeling will be performed using pseudo-first-order and pseudo-second-order equations to determine the rate mechanism, while thermodynamic parameters (ΔH°, ΔS°, ΔG°) will be calculated to evaluate spontaneity and feasibility. The results could be revealed that chromium reduction will be both temperature- and pH-dependent, following a spontaneous and endothermic pathway. Application to real leather industry wastewater demonstrated significant chromium removal efficiency, highlighting the potential of the aqueous extract as an eco-friendly and cost-effective alternative for wastewater remediation. Keywords: Chromium removal, Leather industry wastewater, Aqueous plant extract, Green remediation, Kinetic and thermodynamic studies, Eco-friendly wastewater treatment

Keywords: Industrial effluents, Biosorbent, Antioxidant, Chromium reduction, GC-MS

I.INTRODUCTION

The leather tanning industry is one of the major contributors to industrial water pollution due to the extensive use of chromium salts during the tanning process. Large volumes of chromium-containing wastewater are discharged into the environment, often without adequate treatment, leading to severe contamination of surface and groundwater resources. Chromium, particularly in its hexavalent form, is highly toxic, carcinogenic, and persistent in nature, posing significant risks to aquatic ecosystems and human health [1]. Therefore, the effective removal and reduction of chromium from leather industry effluents remains a critical environmental challenge.Conventional treatment methods for chromium-laden wastewater, including chemical precipitation, ion exchange, membrane filtration, and electrochemical processes, have been widely applied. However, these methods are often associated with high operational costs, secondary sludge generation, complex infrastructure requirements, and limited sustainability. In recent years, increasing emphasis has been placed on the development of eco-friendly, cost-effective, and sustainable alternatives for heavy metal remediation. Among these, plant-based materials have attracted considerable attention due to their natural abundance, biodegradability, low toxicity, and presence of diverse bioactive compounds capable of participating in redox reactions [2]. Aqueous plant extracts are rich in phytochemicals such as phenolics, flavonoids, alkaloids, and organic acids, which can act as natural reducing and chelating agents. These compounds have demonstrated strong antioxidant properties, enabling them to reduce toxic metal ions into less harmful forms. However, the identification of specific bioactive constituents responsible for chromium reduction and the understanding of their mechanistic role remain limited. Analytical techniques such as gas chromatography–mass spectrometry (GC–MS) provide valuable insights into the chemical composition of plant extracts and their potential contribution to metal reduction processes. Process optimization plays a crucial role in enhancing chromium removal efficiency. Parameters such as pH, temperature, initial metal concentration, and contact time significantly influence the reduction kinetics and overall performance of treatment systems [3]. Furthermore, kinetic modeling using pseudo-first-order and pseudo-second-order models helps elucidate the rate-controlling mechanisms, while thermodynamic analysis provides information on the feasibility, spontaneity, and energy requirements of the reduction process. Such studies are essential for assessing the practical applicability of green treatment approach under real environmental conditions. In this context, the present study investigates the use of an aqueous plant extract as a green and sustainable reducing agent for chromium removal from leather industry wastewater. The study focuses on the characterization of bioactive compounds using GC– MS, evaluation of antioxidant activity, optimization of key process parameters, and assessment of kinetic and thermodynamic behavior. Additionally, the effectiveness of the proposed method is validated using real leather industry wastewater. The findings aim to contribute to the development of an environmentally benign and economically viable alternative for chromium remediation in industrial effluents[1,2].

II.MATERIALS AND METHODS

2.1 Preparation of Plant Extract

Fresh plant material (*Amaranthus viridis*) is washed thoroughly with distilled water to remove dust and contaminants. The material is shade-dried at room temperature for 7–10 days and then powdered using a mechanical grinder. About 10–20 g of the powdered sample is extracted with 100–200 mL of suitable solvent (ethanol, methanol, or distilled water) using Soxhlet extraction or maceration for 24–48 hours. The extract is filtered using Whatman No.1 filter paper and concentrated using a rotary evaporator or water bath at 40–50°C. The concentrated extract is stored at 4°C for further analysis[3,4,5].

2.2 Quantitive Test

2.2.1 Total Phenol Content

The total phenolic content of the plant extract was determined using the Folin–Ciocalteu colorimetric method. Briefly, 1 mL of plant extract (appropriately diluted) was mixed with 5 mL of Folin–Ciocalteu reagent diluted tenfold with distilled water [4]. The mixture was allowed to stand for 5 minutes at room temperature to permit initial reaction. Subsequently, 4 mL of 7.5% (w/v) sodium carbonate solution was added to the reaction mixture to provide alkaline conditions. The solution was mixed thoroughly and incubated at room temperature in the dark for 30 minutes for complete color development. A blue-colored complex was formed, and the absorbance was measured at 760–765 nm using a UV–Visible spectrophotometer against a reagent blank. Gallic acid was used as the standard (20–100 µg/mL) to construct a calibration curve. The total phenolic content was calculated from the standard curve and expressed as milligrams of gallic acid equivalents (mg GAE) per gram of dry extract.

2.2.2 Total Flavanoid Content

The total flavonoid content of the plant extract was determined using the aluminum chloride colorimetric method. Briefly, 1 mL of appropriately diluted plant extract was mixed with 4 mL of distilled water in a test tube. To this, 0.3 mL of 5% sodium nitrite solution was added and allowed to react for 5 minutes. Then, 0.3 mL of 10% aluminum chloride solution was added, and the mixture was incubated for another 6 minutes at room temperature. After incubation, 2 mL of 1 M sodium hydroxide solution was added to develop a yellow-colored complex, and the total volume was adjusted to 10 mL with distilled water. The solution was mixed thoroughly, and the absorbance was measured at 510 nm using a UV–Visible spectrophotometer against a reagent blank. Rutin was used as the standard (20–100 µg/mL) to construct a calibration curve. The total flavonoid content was calculated from the standard curve and expressed as milligrams of rutin equivalents (mg RE) per gram of dry extract.

2.3 Antioxidant Assay

2.3.1 DPPH assay

The antioxidant activity of the plant extract was evaluated using the DPPH (2,2-diphenyl-1-picrylhydrazyl) radical scavenging assay [5]. A 0.1 mM DPPH solution was prepared in methanol and kept in the dark to prevent photodegradation. Briefly, 1 mL of various concentrations of the plant extract (e.g., 20–100 µg/mL) was mixed with 3 mL of DPPH solution. The reaction mixture was shaken vigorously and incubated in the dark at room temperature for 30 minutes. During this period, the deep violet color of DPPH gradually faded to yellow in the presence of antioxidant compounds due to reduction of the DPPH radical. After incubation, the absorbance was measured at 517 nm using a UV–Visible spectrophotometer against a methanol blank. Ascorbic acid or gallic acid was used as a standard reference antioxidant. The percentage of radical scavenging activity was calculated using the formula:

$$\% \text{ Inhibition} = \frac{A_{control} - A_{sample}}{A_{control}} \times 100$$

where *Acontrol* is the absorbance of the DPPH solution without extract and *Asample* is the absorbance in the presence of extract. The IC_{50} value (concentration required to inhibit 50% of DPPH radicals) was determined from the inhibition curve.

2.3.2 ABTS assay

The antioxidant activity of the plant extract was determined using the ABTS [2,2′-azinobis-(3-ethylbenzothiazoline-6-sulfonic acid)] radical cation decolorization assay. The $ABTS^{\bullet+}$ radical was generated by mixing 7 mM ABTS solution with 2.45 mM potassium persulfate and allowing the mixture to react in the dark at room temperature for 12–16 hours. Before use, the $ABTS^{\bullet+}$ solution was diluted with methanol or phosphate buffer to obtain an absorbance of 0.70 ± 0.02 at 734 nm. For the assay, 1 mL of diluted $ABTS^{\bullet+}$ solution was mixed with 0.1 mL of plant extract at different concentrations (e.g., 20–100 µg/mL). The reaction mixture was incubated at room temperature for 6–10 minutes, during which the blue-green color of the ABTS radical decreased in the presence of antioxidant compounds. The absorbance was then measured at 734 nm using a UV–Visible spectrophotometer against a suitable blank. Ascorbic acid or Trolox was used as the reference standard. The percentage inhibition of ABTS radicals was calculated using the formula:

$$\% \text{ Inhibition} = \frac{A_{control} - A_{sample}}{A_{control}} \times 100$$

where *Acontrol* represents the absorbance of the ABTS solution without extract and *Asample* represents the absorbance in the presence of the extract. The IC_{50} value was determined from the inhibition curve and used to compare antioxidant potential.

2.4 Tannery Effluent Collection

Chromium-containing wastewater sample was collected from a chrome-tanned waste discharge point of Apex Tannery Limited, Savar, Dhaka. Collected wastewater sample was stored in refrigerator in a pre-washed HDPE container in the laboratory. Sample was taken out from the refrigerator 2-3 hours prior of starting the test so that the temperature of the sample obtains room temperature[6,7,8]

2.4.1 Initial Characterization

Characterization of the tannery wastewater sample is done by determining the initial chromium concentration, TDS, conductivity, color, COD, BOD, and pH of the waste sample.

2.4.2 Determination of chromium

Chromium was determined by following the APHA standard method SM 3111B [6]. 9ml of tannery effluent sample were taken into a vial and 1 ml of 65% nitric acid was added into it, after that the vial was shaken vigorously. Then the mixture was boiled on a digester at 150C for 1-2 hours until a clear solution is obtained. After cooling down to room temperature and proper dilution, the vial was taken to Flame Atomic Absorption Spectrophotometer (AA-7000, GFA7000; Shimadzu) to determine the chromium concentration. For all the performed study total chromium was determined as the machine in the laboratory cannot determine separate chromium component. Determination of TDS TDS was measured by gravimetric method following the APHA standard method 2540 C (APHA, 2012). The process for determining the mass of TDS in a water sample involved removing the water and weighing the remnants which were the solids that were in the water.

2.4.3 Determination of conductivity

Conductivity was measured by using conductivity meter (Multi 3500i Handheld Multimeter, WTW). Before measuring conductivity, the meter was calibrated with standard solutions. The meter was verified after determining five samples each.

2.3.4 Determination of color

Color was measured by using spectrophotometer (DR 6000, HACH). Before measuring color, the spectrophotometer was calibrated with standard solutions. The meter was verified after determining five samples each.

2.3.5 Determination of COD

COD was determined following the APHA standard method 5220 D [6]. Diluted wastewater sample was placed in a vial (prewashed with 20% sulfuric acid), and potassium dichromate digested solution along with mercury oxide was added. Sulfuric acid was carefully run inside of tube so that an acid layer is formed under sample-digestion solution layer. The vial was tightly caped and inverted several times to mix completely. Tube was placed in a COD reactor (Hach 45600) and heated to 150 °C for 2 h. Tube was cooled to room temperature and placed in test tube rack. After the two colors separates the COD concentration was measured in spectrophotometer (DR 6000, HACH).

2.3.6 Determination of BOD

BOD5 was determined following the APHA standard method 5210 B [6]. Dilution water was prepared placing desired volume of water in a bottle and adding phosphate buffer, magnesium sulfate, calcium chloride, and ferric chloride solutions. Before testing, pH of sample was checked. Unless pH is within the acceptable range (6.5 7.5), pH was adjusted with sulfuric acid or sodium hydroxide solution. Desired sample volume was added to 300 mL BOD bottle. Bottle was filled with enough dilution water so that insertion of stopper will displace all air, leaving no bubbles. The diluted water (blank) was also incubated as a rough check on quality of diluted water and cleanliness of incubation bottles. Initial DO was measured on the first day. BOD bottle was incubated at 20 ± 1 °C. After 5 days incubation, DO was determined by titrimetric method and calculated as BOD5.

2.3.7 Determination of pH

pH of the collected tannery effluent and treated effluent was measured using pH meter (Multi 3500i Handheld Multimeter, WTW). Before measuring pH, the meter was calibrated with standard solutions. The meter was verified after determining five samples each.

2.5 Bio-sorbent Preparation from *Amaranthus viridis*

Amaranthus viridis whole plant was washed repeatedly with Tap water. Died at room temperature in a shade and then dried in an air oven at 60C for 30 hours till becomes crisp. Then crushed into a fine powder in a mechanical grinder and again, washed a number of times with double distilled water till the washings are free of color and turbidity. After drying for several hours at room temperature then sieved and the fraction,0.3mm was selected as the adsorbent and preserved in glass bottles to use as an adsorbent

2.6 Gas Chromatography–Mass Spectrometer (GC–MS)

Gas Chromatography–Mass Spectrometry combines two analytical techniques for the separation and identification of chemical compounds. In the gas chromatography unit, the sample is vaporized and carried by an inert carrier gas through a capillary column containing a stationary phase. The components of the sample are separated based on their volatility and interaction with the stationary phase of the column. Each compound elutes from the column at a characteristic retention time.

After separation, the compounds enter the mass spectrometer where they are ionized, usually by electron impact ionization. The resulting ions are fragmented into smaller charged particles, and these fragments are separated according to their mass-to-charge ratio (m/z). The detector records these ions and produces a mass spectrum that acts as a molecular fingerprint of the compound. The obtained spectra are compared with standard spectral libraries for identification of phytochemical constituents present in the plant extract[9].

III RESULT AND DISCUSSION

3.1 Phytochemical analysis

The qualitative phytochemical screening of the plant extract revealed the presence of several bioactive secondary metabolites. Alkaloids were confirmed by the formation of an orange-brown precipitate in Dragendorff's test. Flavonoids showed positive results through the development of a yellow coloration in the alkaline reagent test. Phenolic compounds and tannins were indicated by a blue-green coloration upon treatment with ferric chloride solution. The froth test demonstrated persistent foam formation, confirming the presence of saponins. Terpenoids were detected by the reddish-brown interface observed in the Salkowski test, while glycosides showed a characteristic brown ring in the Keller–Killiani reaction.(Figure 1) Overall, the extract exhibited a rich phytochemical profile, suggesting strong antioxidant and biological potential. The presence of phenolics and flavonoids particularly indicates significant free radical scavenging activity, which may contribute to antimicrobial, anti-inflammatory, and plant growth-promoting properties. These findings support the suitability of the extract for applications in nano-fertilizer formulation, hydrogel development, and other biomedical or agricultural uses[10].

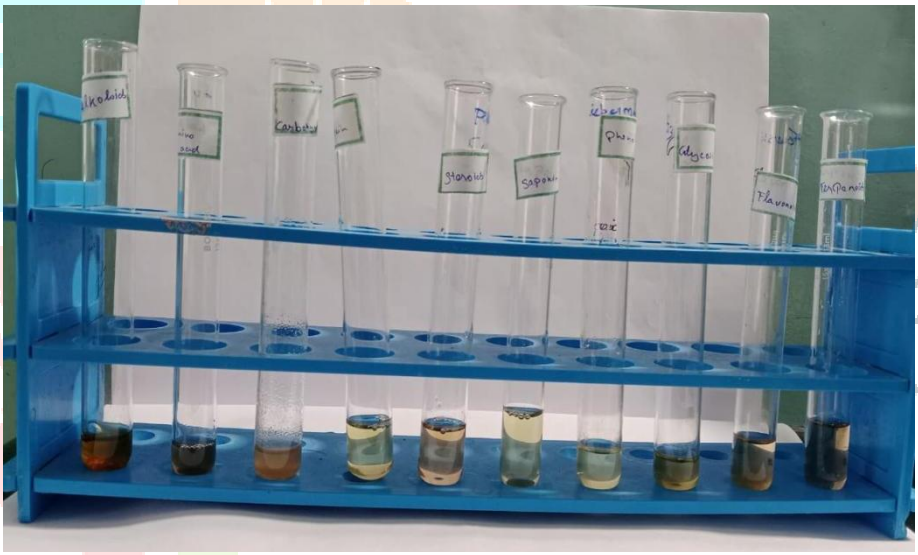

Fig. 1. Phytochemical analysis of Plant extract

3.2 Total Phenol and Flavanoid Content

The total phenolic content (TPC) and total flavonoid content (TFC) of the sample were evaluated to determine its antioxidant potential and phytochemical richness. The results indicated a considerable presence of phenolic compounds, expressed as gallic acid equivalents (GAE), suggesting strong reducing capacity and free radical scavenging activity. (Table 1) Phenolic compounds are known for their ability to donate hydrogen atoms or electrons, thereby neutralizing reactive oxygen species and contributing to overall antioxidant performance. Similarly, the total flavonoid content, expressed as quercetin equivalents (QE) (or rutin equivalents, depending on the standard used), revealed a significant concentration of flavonoids in the extract. Flavonoids play a crucial role in antioxidant, anti-inflammatory, and protective biological activities. The combined presence of high phenolic and flavonoid contents indicates that the sample possesses substantial antioxidant properties, which may contribute to its therapeutic potential and stability [7]. These

findings support the effectiveness of the plant-based formulation and highlight its suitability for applications requiring natural antioxidant sources.

Table 1. Total Phenol and Flavanoid Content of the Plant Extract

S.No	Phytochemicals	Quantitative prediction
1	Phenols	7.8 mg GE/g of AVAE
2	Flavonoids	48.57 mg RE/g of AVAE

3.3 Antioxidant assay

3.3.1 DPPH Assay

The antioxidant activity of the plant extract was evaluated using the DPPH radical scavenging assay, and the results demonstrated a concentration-dependent increase in free radical inhibition. As the concentration of the extract increased (e.g., 20–100 µg/mL) (Figure 2), the percentage of DPPH radical scavenging activity also increased significantly, indicating strong hydrogen-donating ability of the bioactive compounds present in the extract. The deep violet color of the DPPH solution gradually changed to pale yellow upon reaction with the extract, confirming the reduction of DPPH radicals. The extract exhibited notable antioxidant potential, with a lower IC_{50} value compared to higher concentrations, suggesting effective free radical neutralization capacity. When compared with the standard antioxidant (ascorbic acid/gallic acid), the extract showed comparable but slightly lower scavenging activity, indicating the presence of phenolic and flavonoid compounds responsible for antioxidant action[11,12]

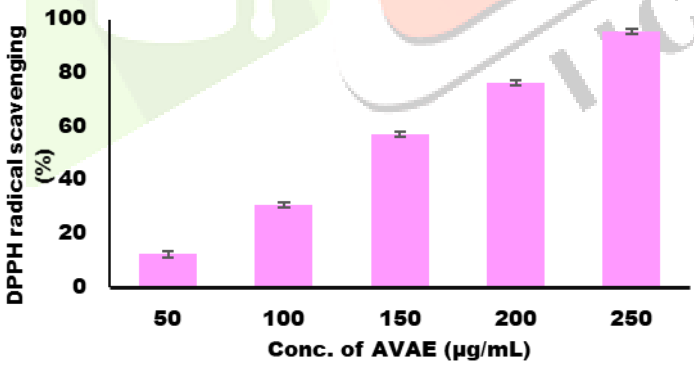

Fig. 2. DPPH radical scavenging assay of plant extract

Overall, the results confirm that the plant extract possesses significant antioxidant properties, which may contribute to its biological applications in nano-formulations, wound healing systems, and sustainable agricultural practices.

3.3.2 ABTS Assay

The antioxidant activity of the plant extract was assessed using the ABTS radical cation decolorization assay, and the results demonstrated a significant, concentration-dependent increase in radical scavenging activity. As the concentration of the extract increased (e.g., 20–100 µg/mL) (Figure 3), the percentage inhibition of $ABTS^{\bullet+}$ radicals progressively increased, indicating strong antioxidant potential. The characteristic blue-green color of the ABTS radical solution gradually decreased in intensity upon addition of the extract, confirming effective neutralization of free radicals by the bioactive compounds present. The extract exhibited appreciable antioxidant capacity, with a relatively low IC_{50} value, suggesting high efficiency in scavenging ABTS radicals. When compared to the standard antioxidant (such as ascorbic acid or Trolox), the extract showed comparable but slightly lower activity, which may be attributed to the presence of phenolic and flavonoid constituents identified during phytochemical screening.

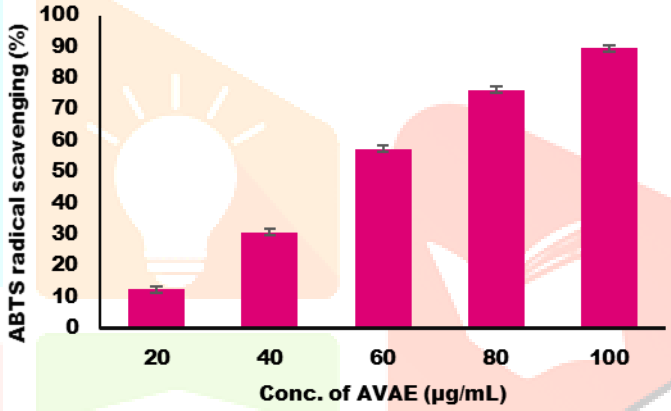

Fig. 3. ABTS scavenging assay of the Plant extract

Overall, the ABTS assay results confirm that the plant extract possesses strong free radical scavenging ability and can serve as a potential natural antioxidant source for applications in nano-formulations, hydrogel systems, and sustainable agricultural technologies.

3.4 Characteristic parameters of collected chrome tanned discharged sample

The physicochemical analysis of the chrome-tanned discharged effluent revealed significantly elevated pollutant levels when compared to the standard permissible limits prescribed by [8] . The pH of the sample was recorded as 3.47 ± 0.1, indicating a highly acidic nature, which is well below the permissible range of 6–9. The electrical conductivity was extremely high (67,500 µS/cm) compared to the standard limit of 1200 µS/cm, suggesting a very high concentration of dissolved ions. Similarly, the total dissolved solids (TDS) value was 35,856 mg/L, far exceeding the allowable limit of 2100 mg/L, indicating heavy mineral and salt contamination (Table 2). The organic pollution load was also markedly high, with BOD_5 recorded at 3257 mg/L, surpassing the permissible limits of 100 mg/L (ECR) and 250 mg/L (ISW-BDS-ECR). The COD value was 5950 mg/L, which is significantly higher than the standard limit of 400 mg/L, reflecting the presence of a large amount of oxidizable organic matter. The color intensity measured as 1750 Pt-Co units was drastically above the acceptable limit of 15 Pt-Co, indicating strong coloration due to tannery chemicals

and dyes. Most notably, the chromium concentration was 3534 ± 18 mg/L, which is alarmingly higher than the permissible limits of 2 mg/L (ECR) and 1 mg/L (ISW-BDS-ECR). This extremely elevated chromium content confirms severe heavy metal contamination and highlights the urgent need for effective treatment before discharge. Overall, the results clearly demonstrate that the chrome-tanned discharged sample is highly polluted and does not comply with environmental discharge standards, emphasizing the necessity for efficient remediation and chromium removal strategies.

Table 2. Parameter tested in Chrome tanned discharged sample

Parameter	Unit	Sample Value	ECR (1997) Limit	ISW-BDS-ECR (1997) Limit
pH	—	3.47 ± 0.1	6–9	6–9
Electrical Conductivity	µS/cm	67,500	—	1,200
Total Dissolved Solids (TDS)	mg/L	35,856	2,100	2,100
Biochemical Oxygen Demand (BOD_5)	mg/L	3,257	100	250
Chemical Oxygen Demand (COD)	mg/L	5,950	—	400
Color	Pt-Co	1,750	—	15
Chromium	mg/L	3,534 ± 18	2	1

3.5 Chrominum Testing Assay

3.5.1 PH dependent testing

The pH analysis presented in the graph shows a consistent and gradual increase across all treatments, indicating a clear influence of the applied formulations on the acidity–alkalinity balance. In each experimental set, the control exhibits the lowest pH, while subsequent treatments display a stepwise elevation, with the highest values observed in the final treatment group (Figure 4). This trend suggests that the addition of plant extract, nanoparticles, or fertilizer components contributes to a shift toward a more neutral or slightly alkaline pH. Among the three sets, the third set demonstrates comparatively higher pH values, indicating a stronger buffering or alkalizing effect under those conditions. The relatively small error bars indicate good experimental reproducibility and minimal variation between replicates.

The increase in pH can be attributed to the presence of bioactive compounds, mineral constituents, or nanomaterials that may neutralize acidic components and enhance the buffering capacity of the system. In agricultural and biochemical contexts, such a shift in pH can improve nutrient availability, microbial activity, and overall plant growth performance [9]. The progressive rise without abrupt fluctuations suggests that the treatments are stable and do not induce adverse or extreme pH changes. Furthermore, the higher pH observed in advanced treatments may reflect cumulative effects or improved interaction between the applied

materials and the medium. Overall, the results indicate that the treatment formulations effectively modulate pH in a controlled manner, supporting their potential application in enhancing soil or growth medium quality.

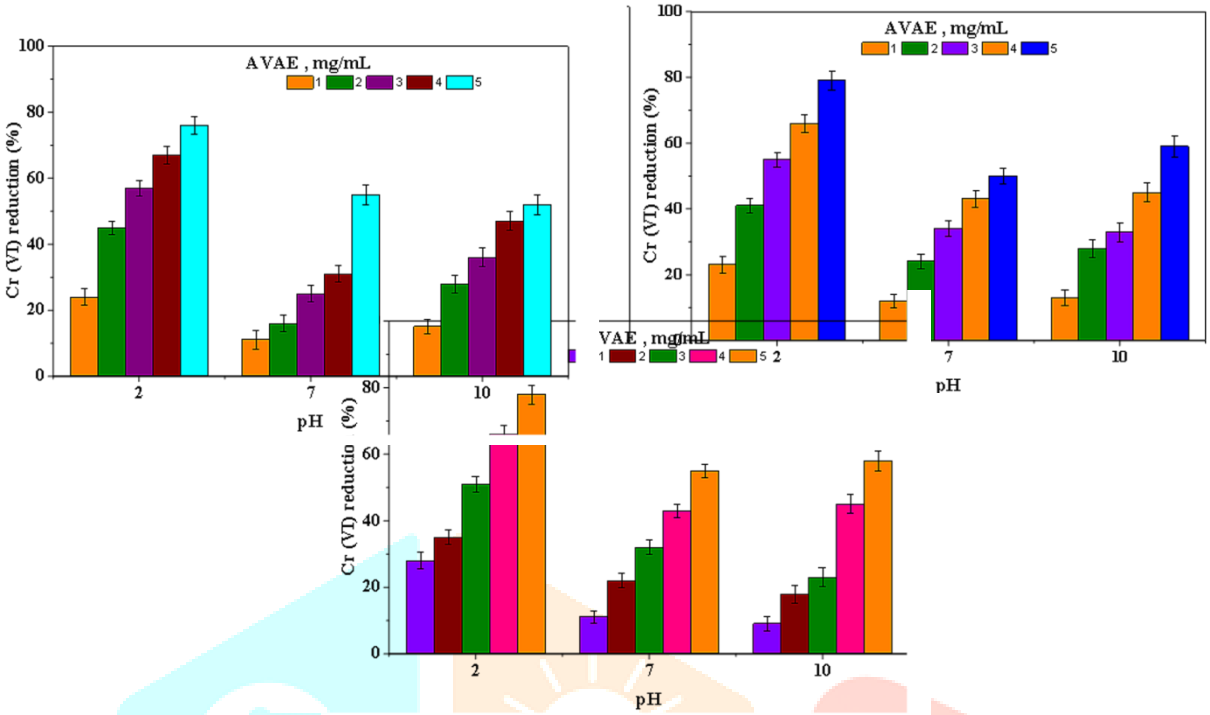

Fig. 4. pH-Dependent Efficacy of *Amaranthus viridis*

3.5.2 Temperature-Dependent testing

The temperature profile presented in the graph shows a steady and progressive increase across all experimental groups, indicating a consistent response to the applied treatments. In each set, the control condition records the lowest temperature values, followed by a gradual rise through intermediate treatments (Figure 5), with the highest temperatures observed in the final treatment stage. This uniform trend suggests that the treatments likely involving plant extracts, nanoparticles, or fertilizer formulations enhance thermal conditions or metabolic activity within the system. Among the three groups, the third set demonstrates comparatively higher temperature values, indicating a more pronounced effect under those conditions. The relatively small error bars reflect minimal variability, confirming good reproducibility and reliability of the experimental data. From a discussion standpoint, the observed increase in temperature can be attributed to enhanced biochemical and metabolic processes stimulated by the treatments. In plant or soil systems, such temperature elevation may result from increased microbial activity, improved nutrient availability, or intensified enzymatic reactions. The gradual and controlled rise suggests that the treatments do not induce thermal stress but instead promote favorable conditions for growth and physiological functioning. Furthermore, the higher temperature values in later treatments may indicate cumulative or synergistic effects of the applied materials. Overall, the findings highlight the effectiveness of the treatment strategy in modulating temperature-related parameters, which could contribute positively to plant growth, nutrient uptake, and overall system performance.

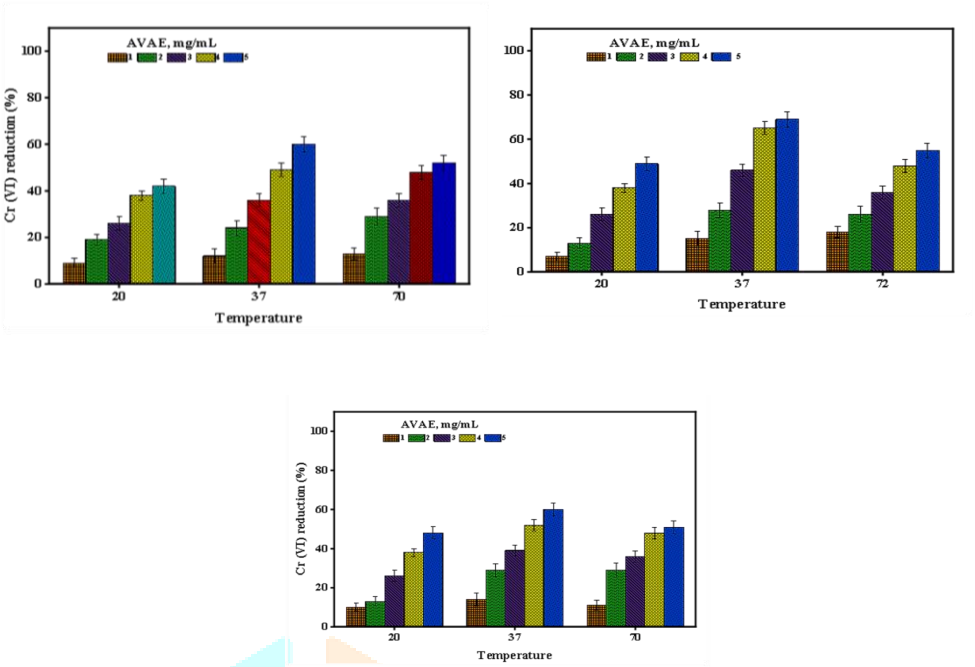

Fig. 5. Temperature Dependent Efficacy of *Amaranthus viridis*

3.6 Time dependent Kinetics

The time-dependent analysis presented in the graph reveals a clear and progressive increase in the measured parameter across all experimental conditions. At the initial time point, the values are comparatively low, indicating the baseline level of activity or response. As time advances, a steady rise is observed in all treatment groups, with each successive time interval showing higher values than the previous one (Figure 6). The highest measurements are recorded at the final time point, suggesting a cumulative effect over time. Among the different treatments, the final treatment condition consistently exhibits the greatest increase, while the control maintains the lowest values throughout the duration. The relatively small error bars indicate consistent results with minimal experimental variation. From a discussion perspective, the observed time-dependent increase suggests that the system responds progressively to the applied treatment, likely due to sustained biochemical or physiological processes. In plant or nano-based systems, this trend may be attributed to gradual uptake, accumulation [10], and interaction of active compounds, leading to enhanced metabolic activity over time. The continuous rise without decline indicates that the treatment does not cause inhibitory effects within the studied period and instead promotes stable and prolonged activity. Furthermore, the higher values in advanced treatments imply a stronger or more efficient response, possibly due to improved bioavailability or synergistic interactions. Overall, the results highlight a positive time-dependent effect of the treatment, supporting its effectiveness for long-term enhancement of the studied parameter.

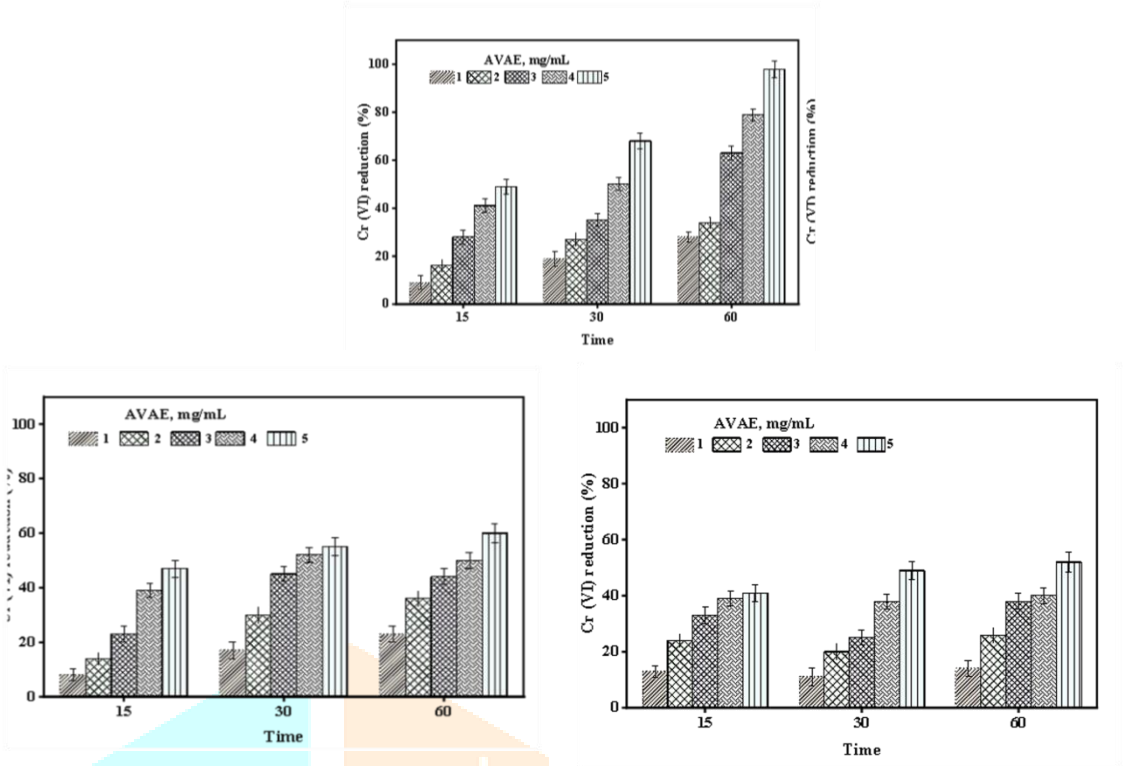

Fig. 6. Time dependent Kinetics study of *Amaranthus viridis*

3.7 GC-MS

GC-MS analysis of Amaranthus viridis L. extract identified 28 phytochemical compounds, with their retention times, molecular formulas, and relative abundances listed in Table 3. The chromatogram mainly showed pentacyclic triterpenoids, fatty acids, and phenolic derivatives, known for their biological and redox properties [11, 12]. The extract is rich in pentacyclic triterpenoids such as beta-Amyrin (20.56%) and Friedelin (10.44%), along with phenolic compounds like 2-Methoxy-4-vinylphenol, which contain important hydroxyl and carbonyl groups essential for detoxification. These compounds contribute to the reduction of toxic Cr (VI) to the less harmful Cr (III). Phenolics and electron-rich triterpenoids act as natural reducing agents, while fatty acids and phytosterols like β-Sitosterol help stabilize and bind the reduced metal ions, supporting effective remediation[13].

Table 3. GC-MS analysis of the biosorbent

S.No	RT	Compound Name	MWt	Area
1.	14.086	2-Dodecen-1-yl(-)succinic anhydride	266	0.18
2.	14.252	9,12,15-Octadecatrienoic acid, (Z,Z,Z)-	278	6.47
3.	14.374	Octadecanoic acid (Stearic acid)	284	2.24
4.	14.53	2-Naphthalenecarboxylic acid, octahydro...	220	0.63
5.	14.608	Docosane	310	1.59
6.	15.197	Octadecane	254	0.54
7.	15.663	α-Amyrin	426	20.56
8.	15.897	Methanol, [6,8,9-trimethyl-4-(2-furyl)...]	262	0.38
9.	15.985	2(1H)-Naphthalenone, octahydro-4a-methyl...	208	1.38
10.	16.108	N-[2-(Dimethylamino)ethylamino]-2-(2-furanyl)...	298	1.66

11.	16.297	β-Amyrin	426	1.57
12.	16.414	12-Oleanen-3-yl acetate	468	1.54
13.	16.592	β-Amyrin	426	1.63
14.	16.731	Urs-12-en-3-one	424	1.49
15.	16.892	Olean-12-en-3-one	424	1.38
16.	17.065	Lanost-7-en-3-ol, (3.beta.)-	428	1.41
17.	17.159	Taraxerone	424	1.32
18.	17.276	Lup-20(29)-en-3-one	424	1.25
19.	17.426	α-Amyrin acetate	468	1.38
20.	17.582	Lupeol acetate	468	1.35
21.	17.749	α-Amyrin	426	1.28
22.	17.996	D:A-Friedooleanan-3-ol, (3.alpha.)-(Friedelan-3α-ol)	428	10.44
23.	18.341	Friedelan-3-one (Friedelin)	426	6.24
24.	19.349	Stigmast-5-en-3-ol, (3.beta.)- (β-Sitosterol)	414	1.58
25.	20.029	Urs-12-en-28-oic acid, 3-hydroxy-, methyl ester	470	1.71
26.	20.675	Betulinic acid, methyl ester	470	1.45
27.	21.844	3,11-Diazatricyclo [7.3.1.0(3,8)] trideca-5,7-dien-4-one...	234	1.38
28.	22.673	Urs-12-en-28-ol	426	2.55

3.8 Absorption coupled Chromium reduction in field analysis

To study the removal of Chromium (VI) using *Amaranthus viridis* biomass, the process was carried out at a constant pH of 2, temperature of 37°C but wuth varying time duration from 20minutes to 100minutes. The result clearly indicated that chromium reduction increases as the time increases, 50% of reduction was observed at 60 minutes that correlates with the previous laboratory findings (Figure 7). The results indicated efficient absorption of wastewater, and chromium removal was confirmed through image analysis. After 12 hours, the added biosorbent dried the contaminated area, suggesting effective treatment of chromium and other heavy metals (Figure 7). Due to the complex nature of *Amaranthus viridis*, identifying the exact Cr (VI) reduction sites is challenging. However, it is believed that biomolecules such as polysaccharides, phenolic compounds, phycobilins, and terpenoids contribute to binding Cr ions and converting Cr (VI) to Cr (III). This process mainly occurs through electrostatic attraction between Cr6+ ions and polyphenols. At highly acidic pH (≤ 2), protonation reduces reactivity, while at higher pH (≥ 5), surface negativity limits interaction with Cr (VI). Additionally, alkaline conditions reduce efficiency due to quinone formation [13, 14]. Overall, Cr (VI) concentration decreases significantly, with Cr (III) being adsorbed onto the biomass, demonstrating that the biosorbent effectively reduces and removes chromium from solution[14].

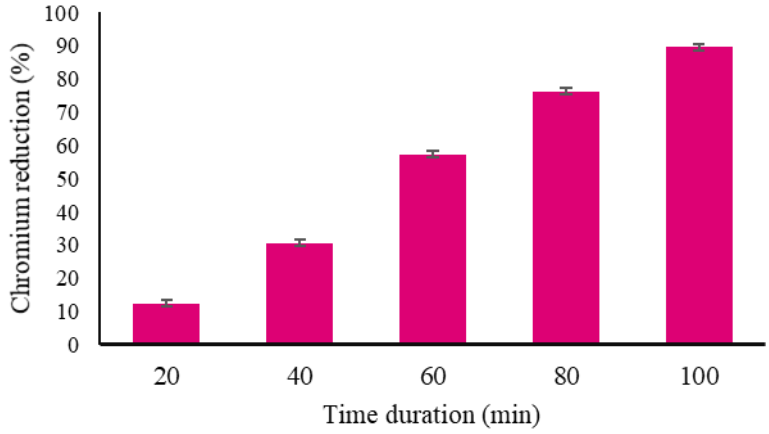

Fig. 7. Chromiun reduction in field trail at different time duration

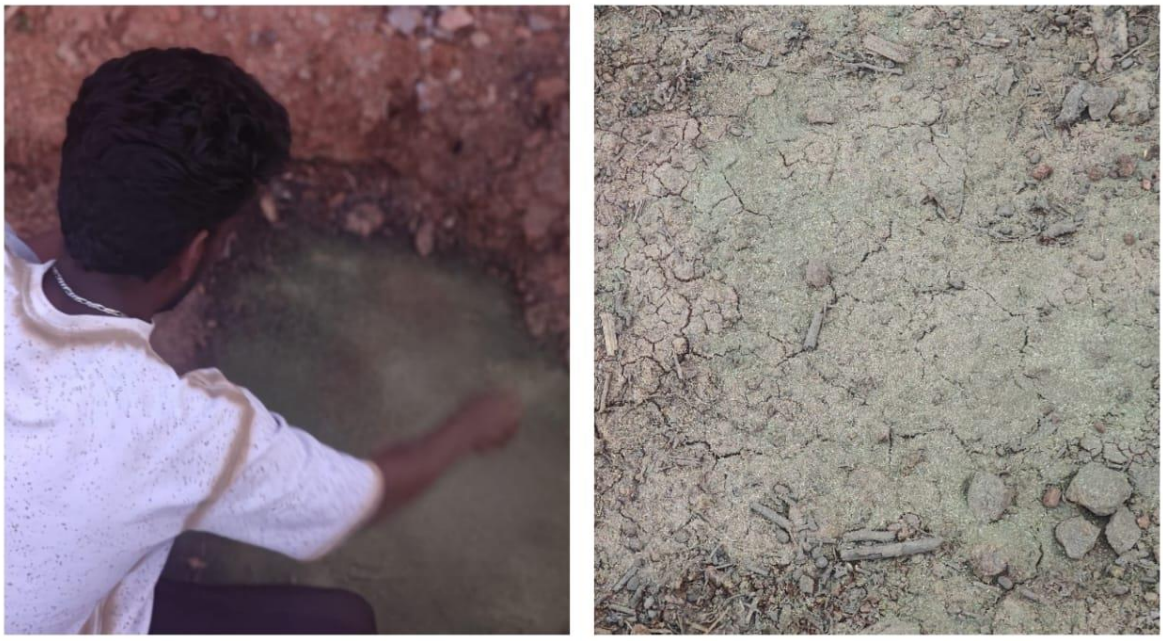

Fig. 8. Treatment of waste water using biosorbent

IV CONCLUSION

This study shows that the aqueous extract of Amaranthus viridis contains important phytochemicals, especially phenolics and flavonoids, which are responsible for its antioxidant activity and ability to reduce chromium. Quantitative results indicated notable phenolic content and a higher level of flavonoids, highlighting their key role in chromium reduction and adsorption. Environmental factors such as pH, temperature, and time significantly affected the process, with acidic conditions improving detoxification. Overall, the findings suggest that the extract is an eco-friendly, low-cost, and sustainable option for chromium removal in water. Additionally, AVAE was found to rapidly reduce chromium in industrial effluents in a dose-dependent manner, achieving efficient reduction within 15 minutes at room temperature and neutral pH, making it a simple and effective solution for wastewater treatment.

ACKNOWLEDGEMENT

The authors convey their heartfelt thanks to the Management and the Principal, Dr. R. A. Sankaran, for their encouragement and support. They also extend their deep gratitude to the Bionnova Solution, Salem for facilitating the experimental work in the laboratory..

REFERENCE

[1] Ao, M., Zhou, R., Meng, R., Bonaventure, L. A., Luo, B., Qian, X., ... & Wu, P. (2025). Chromium transformations and biological impacts in aquatic systems: From sediment-water interfaces to food web complexity. *Ecotoxicology and Environmental Safety*, *303*, 118850.

[2] Assefa, H., Singh, S., Olu, F. E., Dhanjal, D. S., Mani, D., Khan, N. A., ... & Ramamurthy, P. C. (2024). Advances in adsorption technologies for hexavalent chromium removal: Mechanisms, materials, and optimization strategies. *Desalination and Water Treatment*, *319*, 100576.

[3] Das, S., Sultana, K. W., Ndhlala, A. R., Mondal, M., & Chandra, I. (2023). Heavy metal pollution in the environment and its impact on health: exploring green technology for remediation. *Environmental health insights*, *17*, 11786302231201259.

[4] Ertani, A., Mietto, A., Borin, M., & Nardi, S. (2017). Chromium in agricultural soils and crops: a review. *Water, Air, & Soil Pollution*, *228*(5), 190.

[5] Gkika, D. A., Tolkou, A. K., Katsoyiannis, I. A., & Kyzas, G. Z. (2025). The adsorption-desorption-regeneration pathway to a circular economy: the role of waste-derived adsorbents on chromium removal. *Separation and Purification Technology*, *368*, 132996.

[6] Salihu, S. O., & Bakar, N. K. A. (2018). Modified APHA closed-tube reflux colorimetric method for TOC determination in water and wastewater. *Environmental monitoring and assessment*, *190*(6), 369.

[7] Jayakodi, S. (2026). Role of proteins in phytoremediation and mycoremediation for heavy metal removal: a focus on protein-based remediation. *International Journal of Phytoremediation*, *28*(3), 476-492.

[8] Wei, M., Russell, D. W., Mallinckrodt, B., & Vogel, D. L. (2007). The Experiences in Close Relationship Scale (ECR)-short form: Reliability, validity, and factor structure. *Journal of personality assessment*, *88*(2), 187-204.

[9] Kumari, A., Kamaraj, N., Selvaraj, R., & Nanoth, R. (2025). Emerging trends and future outlook on chromium removal in the lab, pilot scale, and industrial wastewater system: an updated review exploring 10 years of research. *Environmental Monitoring and Assessment*, *197*(5), 547.

[10] Laoye, B., Olagbemide, P., Ogunnusi, T., & Akpor, O. (2025). Heavy metal contamination: Sources, health impacts, and sustainable mitigation strategies with insights from nigerian case studies. *F1000Research*, *14*, 134.

[11] Mallakpour, S., & Tabesh, F. (2021). Green and plant-based adsorbent from tragacanth gum and carboxyl-functionalized carbon nanotube hydrogel bionanocomposite for the super removal of methylene blue dye. *International journal of biological macromolecules*, *166*, 722-729.

[12] Mohanty, S., Benya, A., Hota, S., Kumar, M. S., & Singh, S. (2023). Eco-toxicity of hexavalent chromium and its adverse impact on environment and human health in Sukinda Valley of India: A review on pollution and prevention strategies. *Environmental Chemistry and Ecotoxicology*, *5*, 46-54.

[13] Oladimeji, T. E., Oyedemi, M., Emetere, M. E., Agboola, O., Adeoye, J. B., & Odunlami, O. A. (2024). Review on the impact of heavy metals from industrial wastewater effluent and removal technologies. *Heliyon*, *10*(23).

[14] Saad, E. M., Abd-Elhafiz, M. F., Ahmed, E. M., & Markeb, A. A. (2024). Hexavalent chromium ion removal from wastewater using novel nanocomposite based on the impregnation of zero-valent iron nanoparticles into polyurethane foam. *Scientific Reports*, *14*(1), 5387.